Physical sciences

Liquid-crystalline aqueous clay suspensions.

Laurent J. Michot[1], Isabelle Bihannic[1], Solange Maddi[1], Sérgio S. Funari[2], Christophe Baravian[3], Pierre Levitz[4], Patrick Davidson[5].

1. Laboratoire Environnement et Minéralurgie Nancy University CNRS-INPL UMR 7569 BP40 54501 Vandœuvre Cedex France.

2. HASYLAB. NotkeStrasse 85, D-22603, Hamburg, Germany.

3. Laboratoire d'Energétique et de Mécanique Théorique et Appliquée Nancy University UMR 7563 CNRS-INPL-UHP, 2, Avenue de la Forêt de Haye, BP160 54504 Vandœuvre Cedex, France.

4. Laboratoire de Physique de la Matière Condensée UMR 7643 CNRS-Polytechnique Ecole Polytechnique91128 Palaiseau Cedex, France

5. Laboratoire de Physique des Solides UMR 8502 CNRS-Université Paris-Sud Bât 510 91405 Orsay Cedex France.

Corresponding author : Laurent J. Michot

Tel : (33) 3 83 59 62 94

FAX : (33) 3 83 59 62 55.

e-mail : laurent.michot@ensg.inpl-nancy.fr

Abstract: This article demonstrates the occurrence of a true isotropic/nematic transition in colloidal Brownian aqueous suspensions of natural nontronite clay. The liquid-crystalline character is further evidenced by polarized light microscopy and small angle X-ray scattering experiments in the presence and absence of modest external magnetic fields. The complete phase diagram ionic strength/volume fraction then exhibits a clear biphasic domain in the sol region just before the gel transition in contrast with the situation observed for other swelling clays where the sol/gel transition hinders the isotropic/nematic transition. SAXS measurements of gel samples reveal strong positional and orientational orders of the particles proving unambiguously the nematic character of the gel thus clearly refuting the still prevalent "house of cards" model that explains the gel structure by attractive interactions between clay platelets. As such order is also observed in various other swelling clay minerals, this shows a very general behavior that must be taken into account to reach a better understanding of the rheological properties and phase behavior of these systems.

Introduction :

Swelling clay minerals are layered compounds that bear a negative layer charge compensated by interlayer exchangeable cations whose valence and hydration properties control both swelling and colloidal behavior. One of their most important properties is their ability to form yield stress materials when dispersed in water. This feature, extensively used in various industrial applications (drilling fluids, food industry, cosmetic industry…), also plays a major role in many fundamental processes occurring at the Earth's surface such as slipping processes in plate-boundary faults (1-4) or landslide triggering (5-9). For these reasons, numerous studies have focused on the rheology of aqueous clay suspensions with particular emphasis on yield stress, thixotropy, and aging (10-15). However, most studies neglect a key-feature of clay minerals, i.e., their anisotropic shape. Actually, due to their high aspect ratio typically ranging between 25 and 1000, these materials should very likely form liquid-crystalline phases (16), such as those observed for rod-like clay particles such as imogolite in aqueous media (17) or organophilic sepiolite clay particles in non aqueous solvents-(18). A phase transition was indeed observed by Langmuir as early as 1938 in suspensions of natural hectorite swelling clay

(19)*[*]. However, all subsequent studies failed to reproduce this crucial observation and give evidence of a clear thermodynamic liquid-crystalline order but instead revealed a dominant gel formation (20). Such behavior is observed for both highly polydisperse natural samples (21) and synthetic monodisperse ones (22). The structure and formation mechanisms of the gel are still under debate. Indeed, even though some of the gel features indicate nematic ordering (23, 24), no true thermodynamic nematic order was ever clearly evidenced[t]In this manuscript, we show that aqueous suspensions of natural clay minerals can really exhibit a true isotropic/nematic transition, that the nematic phase displays strong orientational order, and that it can be aligned in modest magnetic fields, a distinctive feature of liquid-crystalline phases.

Results and discussion.

The clay mineral used in this study is a nontronite from Southern Australia (25). Nontronite is a naturally occurring swelling dioctahedral clay mineral related to the montmorillonite-beidellite series in which most aluminum atoms are replaced by iron (III) ions. The structural formula of the nontronite used in the present study was recently refined (26) as $(Si_{7.55}Al_{0.16}Fe_{0.29})$ $(Al_{0.34}Fe_{3.54}Mg_{0.05})$ $O_{20}(OH)_4$ $Na_{0.72}$. Based on unit-cell parameters, its density can be estimated around 3.0g/cm^3. After purification and size fractionation, four different fractions were obtained. The results presented in this report deal with the third size fraction in which the elementary lath-shaped nontronite particles have an average length and width of 147nm and 52 nm with standard deviations of 40% and 38%, respectively. Suspensions prepared with this size fraction are stable over years whereas in higher size fractions, sedimentation starts occurring after a few weeks, which affects the phase diagram (27).

---

[*] In a footnote p877 of his original paper Langmuir clearly mentions that the phase separation was non reproducible. Furthermore, some of the features of the phase transition observed by Langmuir are a bit awkward. Indeed, the transition appears within the gel phase, with the isotropic phase separating out of the birefringent material. Furthermore, the relative proportion of isotropic phase increases with the total concentration, which is the contrary of what should be observed in the case of an isotropic/nematic phase transition.

[t] One of us (P.D.) did observe some phase separation in a couple of laponite samples and mentioned it in reference (23). However, as in the case of Langmuir's experiments the observation was not reproducible and none of us working with laponite samples have been able since to re-observe such a phase separation.

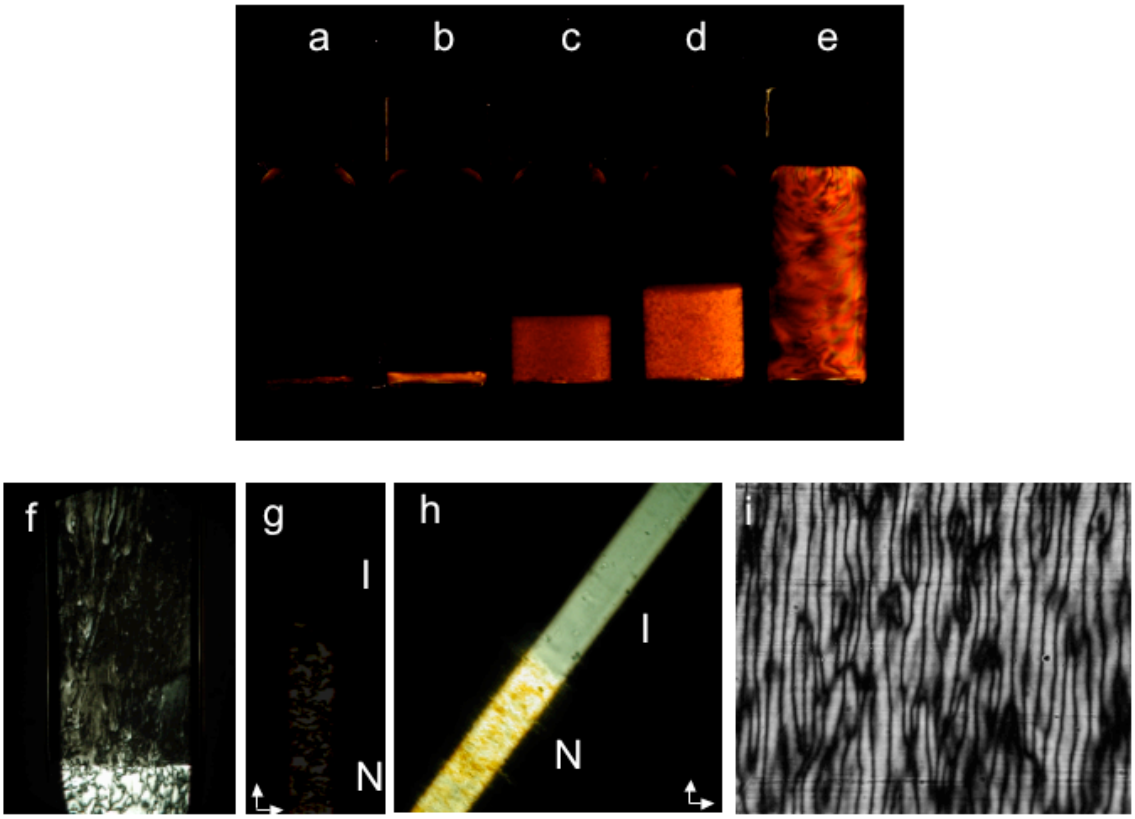

Figure 1. (**a-e**) Naked-eye observation of the samples. 2 ml vials filled with aqueous suspensions of sodium nontronite (IS 10^{-4} M), observed between crossed polarizers (the isotropic phase in **a** to **d** appears dark). **a,** isotropic liquid sample at a volume fraction ϕ = 0.5%. (The small bright line observed at the bottom of the vial is due to a reflection on the curved bottom.) **b,** onset of the phase separation at ϕ = 0.61% **c,** biphasic sample at ϕ = 0.67%. **d,** biphasic sample at ϕ = 0.72%. **e** birefringent gel at ϕ = 1%. (**f**) Polarized-light optical microscopy observations of a nontronite sample (ϕ = 0.7%, ionic strength 10^{-3} M) at the onset of phase separation. (**g-h**) Polarized-light optical microscopy observations of a biphasic sample of a nontronite suspension (ϕ = 0.7%, IS 10^{-3} M) held in a flat capillary submitted to a horizontal 1 T magnetic field. (I: isotropic phase; N: nematic phase; the white arrows show the directions of the polarizers) **g**) extinction conditions: the capillary is barely visible because its axis is parallel to that of the polarizer. **h**) Maximum transmission conditions. The nematic phase is almost uniformly bright because there are only very few defects left. The isotropic phase is not dark due to its large magnetic-field-induced anisotropy. **i**) Transient hydrodynamic instability observed upon a sudden change of magnetic field direction for a nontronite suspension (ϕ = 0.7%, IS 10^{-3} M) held in a flat capillary.

Naked eye observations in polarized light of vials filled with suspensions of increasing volume fractions (at a fixed ionic strength of 10^{-4} M) reveal the following features: (i) At volume fractions $\phi <$ 0.6 %, the suspensions are isotropic liquids (Figure 1a) and exhibit flow birefringence for $\phi \geq$ 0.2%. (ii) At $0.6\% < \phi < 0.8\%$, the suspensions are biphasic with a clear phase separation between a denser birefringent phase at the bottom and an isotropic one at the top (Figure 1 b, c, d). As expected, the proportion of birefringent phase gradually increases with the overall clay volume fraction. It must be emphasized that this represents the first clear-cut and reproducible observation of isotropic/nematic phase separation in aqueous suspensions of natural clay minerals. In contrast with all previous studies, these clay suspensions then reach the isotropic/nematic transition line at thermodynamic equilibrium before gelling. (iii) At $\phi \geq 0.83\%$, the suspensions are birefringent gels (Figure 1e), which means that the sol/gel transition actually occurs at a volume fraction only slightly larger than the nematic edge (0.8%) of the biphasic region. The phase separation is also readily observed by polarized light microscopy (Figure 1f). A few weeks after sample preparation, birefringent droplets are clearly visible in the top isotropic phase; they slowly sediment and coalesce to form the nematic phase. The phase separation is complete after a few months. Similar phenomena are observed with nontronites of size 4. This nematic phase displays a typical threaded texture and the detection of flickering reveals that the suspensions are Brownian.

Due to the presence of ferric iron in the octahedral layer, nontronite suspensions are fairly sensitive to magnetic fields, as shown by Figure 1g and 1h that illustrate the strong alignment of the nematic phase submitted to a 1 T magnetic field. This interesting feature, typical of liquid-crystalline phases, proves that this nematic sample is a fluid rather than a gel of appreciable yield stress. The magnetic field can even be used to micro pattern the orientation of the clay platelets by exploiting a classical transient hydrodynamic instability observed upon a sudden change of field direction (Figure 1i) (26). The period of the modulation can easily be tuned by adjusting the magnetic-field intensity.

A similar evolution with volume fraction is also obtained for an ionic strength of 10^{-3} M. In contrast, at 5.10^{-3} M, no phase separation was observed and the system evolves directly from isotropic liquid to birefringent gel. The complete phase diagram of this nontronite size fraction is presented in Figure 2. At low ionic strength the biphasic domain is tilted towards larger volume fractions (29),

revealing that the system is dominated by repulsions. In contrast, at higher salt concentrations, the sol-gel transition line displays a negative slope and crosses the biphasic region. Such a shape is similar to what was observed in the case of laponite (22). The complete phase diagram where the sol-gel line meets the flocculation line at high ionic strength, suggests that this evolution is likely related to micro-flocculation processes. The shape of rheological flow-curves measurements confirms this interpretation as the viscosity of liquid samples, at high ionic strength, increases at low shear stress. Furthermore, in this region of the phase diagram, significant aging effects are observed, which once again can be linked to microflocculation events that clearly deserve further investigation.

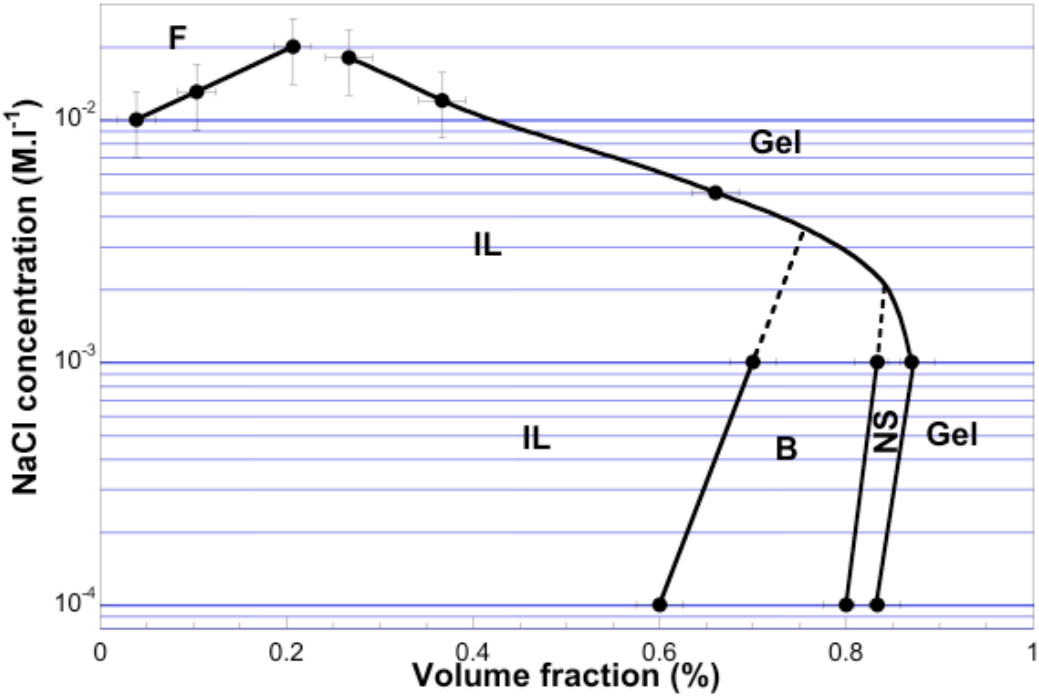

Figure 2. Phase diagram of sodium nontronite suspensions. Upon increasing volume fraction, the suspensions first form an isotropic liquid (IL), then enter a biphasic regime (B) followed by a small region of nematic sol (NS) and finally form birefringent gels. The line between gel and liquid was determined by oscillatory shear measurements. At high salt concentration, the presence of flocs (F) was checked out by visual observation.

On the basis of published statistical physics models and numerical simulations, neglecting polydispersity and electrostatic effects, and considering an average particle diameter of ~ 100 nm, a rough estimated value of ~ 2 % can be obtained for the volume fraction corresponding to the

isotropic/nematic transition (30). In spite of such crude simplifications, this predicted value compares rather well with the experimental one (0.6-0.8 %). Since models and simulations are based on excluded-volume particle interactions only, the experiments reported here strongly suggest that attractive forces, often mentioned to describe clay suspensions, are irrelevant for the onset of nematic ordering at low ionic strength.

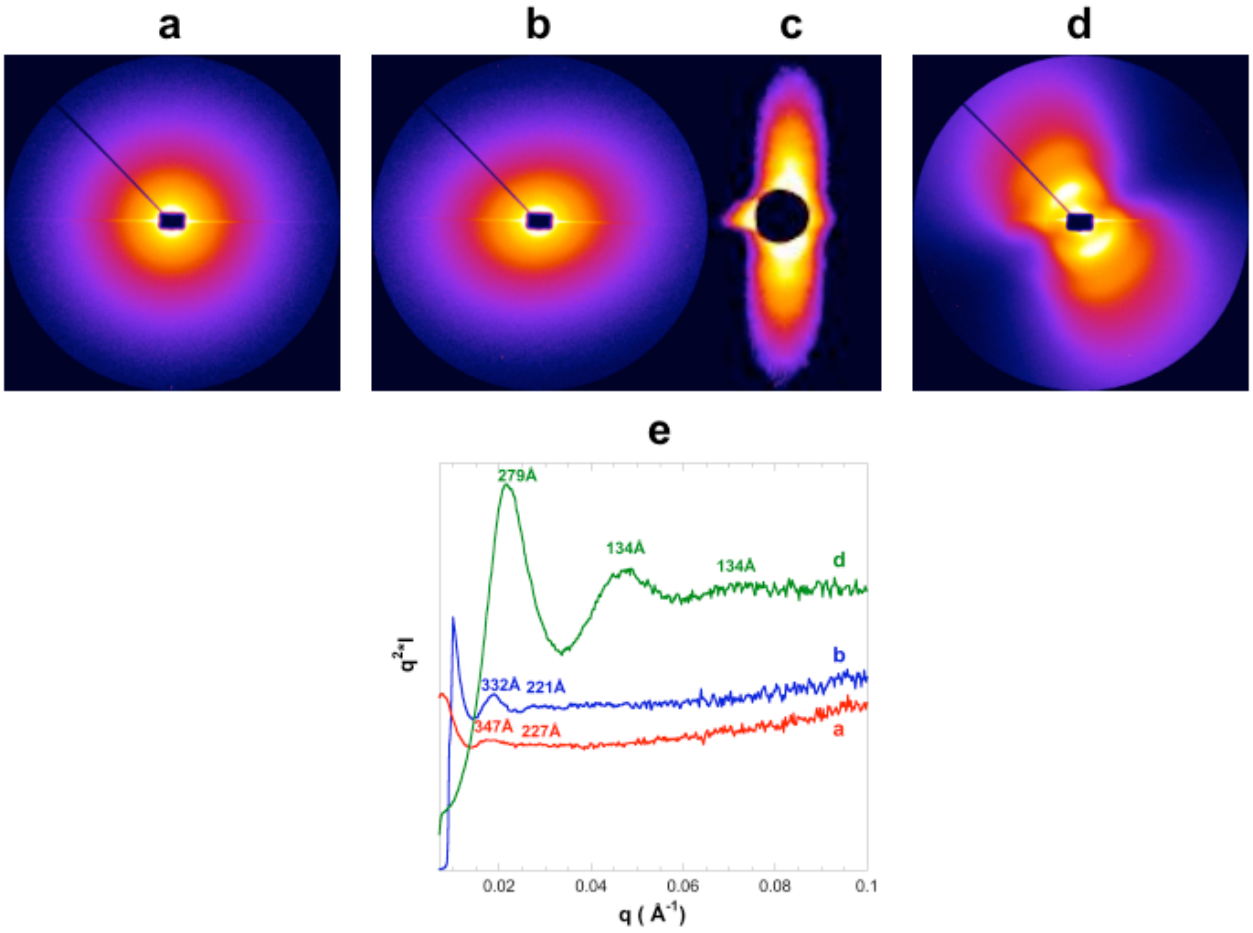

Figure 3. Small-angle X-ray scattering studies. **a**) two-dimensional SAXS pattern of the isotropic phase of a nontronite suspension (ϕ = 0.7%, IS 10^{-3} M) **b**) SAXS pattern of the nematic phase of the same suspension **c**) SAXS pattern of the nematic phase of the same suspension aligned in a magnetic field of 1 Tesla. **d**) SAXS pattern of a gel sample (ϕ = 3%, IS 10^{-3} M). **e**) Plots of $I*q^2$ vs q corresponding to patterns a, b and d. For a and b, the first diffuse peak is too close to the beamstop and is not observed. The intensity of pattern d was divided by 2 for enhanced readability.

The structures of the suspensions were further analyzed by small angle X-ray scattering (SAXS) experiments. Very dilute isotropic suspensions showed a scattering intensity, I monotonously decreasing with increasing scattering vector modulus q as $I \sim q^{-2}$, proving the bidimensional nature of the scattering objects. At larger volume fractions, SAXS patterns display correlation peaks due to short-range positional (i.e. "liquid-like") order of the clay platelets. Typical patterns obtained from the isotropic and birefringent parts of a biphasic sample, are presented in Figure 3a and 3b. The anisotropic character of the birefringent phase is visible and, together with the absence of sharp Bragg reflections, proves its nematic nature. However, the pattern of Figure 3b indicates a very poorly aligned "powder" sample, with a distribution of almost randomly oriented nematic domains. In contrast, when submitted to a magnetic field (Figure 3c), in agreement with optical observations (Figure 1g), the anisotropy of the SAXS pattern is very pronounced, revealing a very strong orientation of nontronite particles. The diffuse-peak positions (d) are the same for both the "powder" and aligned nematic phases, with distances d around 70 nm between clay platelets. In the gel phase (Figure 3d), highly anisotropic SAXS patterns were recorded from samples aligned by the shear-flow achieved when the suspensions were gently centrifuged into the capillaries.

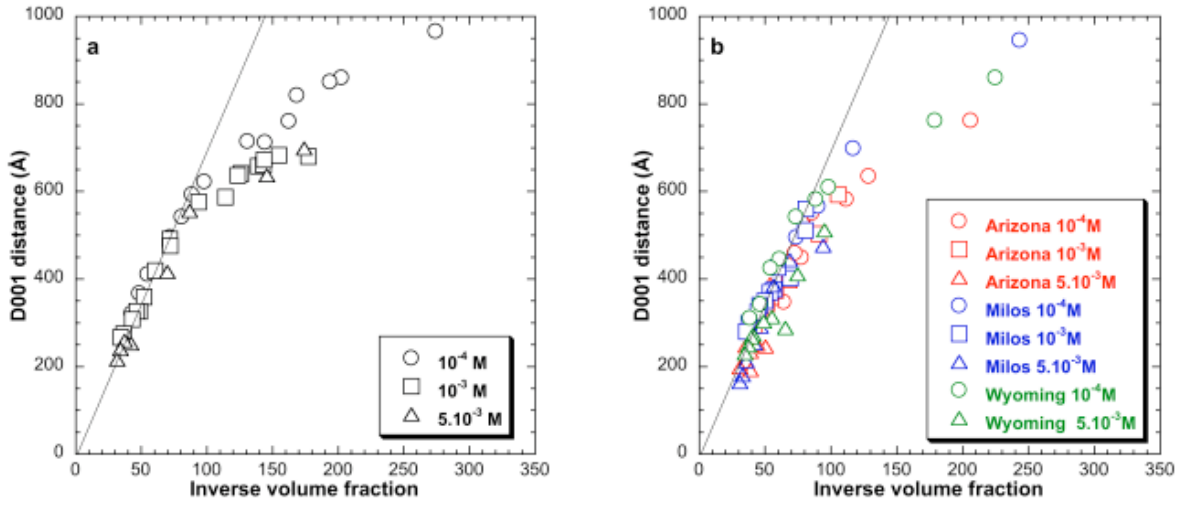

Figure 4. Plots of the average interparticle distances versus inverse volume fraction. The straight line corresponds to 1-dimensional swelling $d = t/\phi$ where $t \approx 0.7$ nm is the thickness of a single clay sheet. **a**) nontronite suspensions **b**) suspensions of montmorillonites from Arizona, Milos, and Wyoming.

The evolution of d with inverse volume fraction (Figure 4a) displays a first regime, for $\phi > 1.1$ %, where d is proportional to $1/\phi$. Such behavior ($d = t/\phi$ where t is the layer thickness) is typical of

the one-dimensional swelling of a pure lamellar phase (31) and therefore suggests a strong lamellar local order of the platelets in the nematic phase. The slope obtained in this regime is $t = 0.70 \pm 0.05$ nm, a value very close to the thickness of a single clay sheet (0.8 nm), proving that the layers are perfectly exfoliated in suspension. The nematic phase then appears as resulting from the orientation of individual charged clay platelets, which is different from the situation encountered for positively charged layered double hydroxides (32) where a phase transition was observed for much thicker stacks of platelets. The linear regime, observed in the nematic phase, ends close to the limit of the biphasic region. There, a crossover occurs towards another regime at lower volume fraction (33) where the distance scales as $\phi^{-1/3}$, suggesting isotropic volume swelling.

Such an evolution of distance versus volume fraction is not specific to nontronite but is also observed for all the size-fractionated swelling clays of similar size that we have investigated (Milos (Greece) Arizona and Wyoming montmorillonites) which points to a very general behavior of smectites, in terms of positional short-range order (Figure 4b). The clear-cut evidence of a first-order isotropic/nematic transition in nontronite suspensions, reported here, therefore strongly suggests that the birefringence of smectite clay gels is indeed the sign of long-range orientational order. In this context, at volume fractions larger than about 1 %, the shear-thinning, non-linear rheological properties of clay suspensions should be discussed in relation to their nematic order and not according to the "house of cards" models that assumes a connected network of interacting clay platelets. Such a feature must then definitely be taken into account for any future modeling of the rheological behavior of clay minerals suspensions both for industrial applications and natural processes.

A puzzling issue is how clay particle properties (dimensions, polydispersity, electric charge, flexibility…) control gelation or liquid-crystalline formation. In the case of the nontronite used in this study, upon increasing volume fraction, the isotropic/nematic transition is observed before gelation whereas suspensions of other clay minerals exhibit gelation before any phase transition takes place. The behavior of nontronite might be assigned to its lath-shape and we are currently developing model calculations and simulations to explore in detail such an assumption. In any case, besides their relevance to the understanding of the rheological behavior of swelling clay minerals, the features revealed in the present paper should strongly contribute to improve our knowledge of the phase behavior of charged anisotropic colloids.

Material and methods.

Clay preparation: The clay sample was ground, exchanged three times in 1 M NaCl and washed by dialysis using ultrapure water until a conductivity < 5μS was obtained. The suspensions were then placed in Imhoff cones for 24 hours in order to discard the major mineralogical impurities (iron oxide and feldspar, mainly). Size fractionation procedures were then applied by centrifuging the stock suspension under different gravitational fields (7000g, 17000g, and 35000g). The supernatant obtained after centrifugation at the highest speed was concentrated by rotoevaporation. Using such a procedure, four size fractions referred to as sizes 1 to 4 were obtained. Mineralogical purity was checked by X-ray diffraction and infrared spectrometry whereas sizes were determined by transmission electron microscopy. The average length and width of sizes 1 to 4 were then (700nm,140nm), (360nm,90nm) (150nm,50nm) and (100nm,45nm) with polydispersities of 50, 40, 38, and 35 % , respectively. The same procedure was applied to montmorillonite samples from Arizona, Milos and Wyoming. Their respective structural formulae can be written as $(Si_{7.95},Al_{0.05})(Al_{2.85}, Mg_{1.07}, Fe_{0.17})O_{20}(OH)_4\ Na_{1.11}$, $(Si_{7.74},Al_{0.26})(Al_{3.0}, Mg_{0.54}, Fe_{0.46})O_{20}(OH)_4\ Na_{0.79}$ and $(Si_{7.76},Al_{0.24})(Al_{3.06}, Mg_{0.48}, Fe_{0.46})O_{20}(OH)_4\ Na_{0.77}$. The respective average sizes of the samples described in the present study (size 3) are 50, 55 and 75 nm and the sheets exhibit very irregular shapes.

Samples at different volume fractions were prepared by osmotic stress using either Dextran or Polyethyleneglycol solutions and Visking dialysis membranes with a cut-off value of 14000 Da. Ionic strength was fixed in the reservoir, to avoid problems related to the Donnan effect.

Rheological measurements were carried out on a TA 2000 instrument. Oscillatory shear measurements were performed to determine the elastic (G') and viscous (G'') modulus of the sample, which were further used to locate the mechanical transition between sol and soft solid, the limit being taken when G' ≈ G''. Additional flow measurements were also carried out in controlled shear-rate mode.

Most small angle X-ray scattering experiments were carried out on beamline A2 at Hasylab, Hamburg using a fixed wavelength of 0.15 nm and a sample to detector distance of 3 m. Bidimensional scattering patterns were collected on a CCD camera and the curves intensity vs q ($q = 4\pi\sin\theta/\lambda$, where 2θ is the scattering angle and λ the wavelength) were obtained by integrating the data in the direction of the anisotropic pattern. Additional SAXS experiments were performed with an in-house setup, using a wavelength of 0.154 nm, a sample to detector distance of 1 m, and a 1 T permanent magnet. All samples were held in cylindrical Lindeman glass capillaries of 1 mm diameter.

Polarized-light microscopy observations were performed with an Olympus microscope and the samples were held in flat glass capillaries (Vitrocom, NJ, US).

Acknowledgements: Support of beamtime at Hasylab by the European Community - Research Infrastructure Action under the FP6 "Structuring the European Research Area" Programme (through the Integrated Infrastructure Initiative "Integrating Activity on Synchrotron and Free Electron Laser Science") Contract RII3-CT-2004-506008 is gratefully acknowledged.

References:

1. Barnes, P.M.., Nicol, A., Harrison, T. (2002) Geol. Soc. Am. Bull. **114**, 1379-1405.
2. Saffer, D.M., Frye, K.M., Marone, C. Mair, K. (2001) Geophys. Res. Lett. **28**, 2297-2300.
3. Mochozuki, K., Nakamura, M., Kasahara, J., Hino, R., Nishino, M., Kuwano, A., Nakamura, Y., Yamada, T., Shinohara, M., Sato, T. et al. (2005) J. Geophys. Res. Solid Earth **110**, 1-16.
4. Matsuda, T., Omura, K., Ikeda, R. Arai, T., Kobayashi, K. Shimada, K. Tanaka, H., Tomita, T, Hirano, S. (2004) Tectonophysics **378**, 143-163.
5. Biscontin, G., Pestana, J.M., Nadim, F. (2004) Mar. Geol. **203**, 341-354.
6. Wan, Y.S., Kwong, J. (2002) Engng Geol. **65**, 293-303.
7. Hungr, O., Evans, S.G., Bovis, M.J., Hutchinson, J.N. (2001) Environ. Engng Geosci. **7**, 221-238.
8. Kerle, N., de Vries, B.V., Oppenheimer, C. (2003). Bull. Volcanol. **65**, 331-345.
9. Waythomas, C.F., Miller, T.P., Beget, J.E. (2000) J. Volcanol. Geoth. Res. **104,** 97-130.
10. Coussot, P., Nguyen, Q.D., Huynh, H.T., Bonn, D. (2002) Phys. Rev. Lett. **88,** art n° 175501.
11. Abou, B., Bonn, D., Meunier, J. (2003) J. Rheol. **47**, 979-988.
12. Bandyopadhyay, R. Liang, D., Yardimci, H., Sessoms, D.A., Borthwick, M.A., Mochrie, S.G.J., Harden, J.L., Leheny, R.L. (2004) Phys. Rev. Lett. **93,** art n° 228302
13. Bekkour, K. Leyama, M., Benchabane, A., Scrivener, O. (2005)) J. Rheol **49**, 1329-1345 (2005).
14. Martin, C., Pignon, F., Piau, J-M, Magnin, A., Lindner, P., Cabane, B. (2002) Phys. Rev. E **66,** 021401.
15. Knaebel, A., Bellour, M., Munch, J-P., Viasnoff, V., Lequeux, F., Harden, J.L. (2003) Phys. Rev. E **67,** 031405.
16. Davidson, P., Gabriel, J-C, P. (2005) Curr. Opin. Colloid Interface Sci. **9,** 377-383.
17 Kajiwara, K., Donkai, N., Hiragi, Y., Inagaki, H. (1986) Makromol. Chem**. 187,** 2883-2893.
18 Zhang, Z.X., Van Duijneveldt, J.S. (2006) J. Chem. Phys. **124,** 15910.
19. Langmuir, I. (1938). J. Chem Phys. **6,** 873-896.
20. Van der Beek, D., Lekkerkerker, H.N.W. (2003). Europhys. Lett. **61,** 702-707.
21. Michot, L.J., Bihannic, I., Porsch, K., Maddi, S., Baravian, C., Mougel, J. Levitz, P. (2004) Langmuir **20,** 10829-10837.
22. Mourchid, A., Delville, A., Lambard, J., Lécolier, E., Levitz, P. (1995) Langmuir **11,** 1972-1950.
23. Gabriel, J.C.P., Sanchez, C., Davidson, P. (1996) J. Phys Chem **100,** 11139-11143.
24. Lemaire, B.J., Panine, P., Gabriel, J.C.P., Davidson, P. (2002) Europhys. Lett. **59**, 55-61.
25. Keeling, J.M., Raven, M.D., Gates, W.P.(2000) Clays Clay Min. **48,** 537-548.
26. Gates, W.P., Slade, P.G., Manceau, A., Lanson, B. (2002) Clays Clay Min **50,** 223-239.
27. Van der Beek, D., Lekkerkerker, H.N.W. (2004). Langmuir **20,** 8582-8586.
28 Srajer, G., Fraden, S., Meyer, R.B. (1989) Phys. Rev. A **39,** 4828-4834.
29. Fraden, S. Maret, G. Caspar, D.L.D. Meyer, R.B. (1989) Phys. Rev. Lett., **63,** 2068.
30. Bates, M.A.; Frenkel, D. (1999). J. Chem. Phys. **110,** 6553-6559.
31. Gabriel, J.C.P.; Camerel, F.; Lemaire, B.J.; Desvaux, H.; Davidson, P.; Batail, P. (2001) Nature **413,** 504-508.
32 Liu, S., Zhang, J., Wang, N., Liu, W., Zhang, C., Sun, D. (2003) Chem. Mater. **15,** 3240-3241.
33. Ramsay, J.D.F.; Lindner, P. (1993) J. Chem. Soc. Faraday Trans. **89**, 4207-4214.